Scientific Research Publishing

Engineering, 2025, 17(1), 1-18
https://www.scirp.org/journal/eng
ISSN Online: 1947-394X
ISSN Print: 1947-3931

Erratum to "Rock Fragmentation Classification Applying Machine Learning Approaches" [Engineering, 15 (2023) 378-395]*

Samaneh Liaghat, Nadhir Al Ansari

Environmental and Natural Resources Engineering Department, Luleå University of Technology, Luleå, Sweden
Email: samaneh.liaghat@associated.ltu.se

How to cite this paper: Liaghat, S. and Al Ansari, N. (2025) Erratum to "Rock Fragmentation Classification Applying Machine Learning Approaches" [Engineering, 15 (2023) 378-395]. *Engineering*, **17**, 1-18.
https://doi.org/10.4236/eng.2025.171001

Received: November 19, 2024
Accepted: January 10, 2025
Published: January 13, 2025

Abstract

The nature of rock fragmentation affects the downstream mining processes like loading, hauling, and crushing the blasted rock. Therefore, it is important to evaluate rock fragmentation after blasting for choosing or designing optimal strategies for these processes. However, current techniques of rock fragmentation analysis such as sieving, image-based analysis, empirical methods or artificial intelligence-based methods entail different practical challenges, for example, excessive processing time, higher costs, applicability issues in underground environments, user-biasness, accuracy issues, etc. A classification model has been developed by utilizing image analysis techniques to overcome these challenges. The model was tested on about 7500 videos of load-haul-dump (LHD) buckets with blasted material from Malmberget iron ore mine in Sweden. A Kernel-based support vector machine (SVM) method was utilized to extract frames comprising loaded LHD buckets. Then, the blasted rock in the buckets was classified into five distinct categories using the bagging *k*-nearest neighbor (KNN) technique. The results showed 99.8% and 89.8% accuracy for kernel-based SVM and bagging KNN classifiers, respectively. The developed framework is efficient in terms of the operation time, cost and practicability for different mines and variate amounts of rock masses.

Keywords

Rock Blasting, Load Dump Haul, Image Analysis, Artificial Intelligence, Mine Productivity

*The original version of this article (Liaghat, S., Al Ansari, N. and Iravani, A. (2023) "Rock Fragmentation Classification Applying Machine Learning Approaches", Engineering, 15, 378-395. https://doi.org/10.4236/eng.2023.156030) was published as some results data reported mistakenly. The authors wish to correct the errors.

1. Introduction

Fragmenting *in-situ* rock mass into smaller pieces is a fundamental process in mining, facilitating faster loading and transportation of smaller fragments to downstream operations compared to larger boulders [1]. Drilling and blasting are often preferred for rock excavation due to their efficiency in handling large volumes of hard rock [2]. This process involves using explosives to fragment rock masses, and its success depends on factors like explosive type, drilling parameters, and rock mass characteristics [3]. Effective blasting reduces downstream costs related to loading, hauling, and crushing, making it essential to evaluate blast outcomes systematically [4]. Rock fragmentation, which measures the size distribution of blasted rock, plays a crucial role in optimizing the mining process and minimizing overall costs [5] [6].

Fragmentation impacts production rates and equipment performance, influencing loading, transport, and crushing costs [7] [8]. Studies have explored fragmentation's role in maximizing mineral extraction, improving drilling tool selection, optimizing blasting strategies, and refining mill operations [9]-[11]. Thus, reliable fragmentation prediction is critical for blast optimization [12] [13].

Fragmentation assessment methods include direct approaches like sieving analysis and indirect methods such as empirical, observational, and image-based techniques [2] [12]-[17]. While sieving analysis is accurate, it is time-intensive and impractical for routine use [7]. Observational methods, reliant on manual classification, are prone to bias and limited accuracy [13]. Empirical models, such as Swebrec and Rosin-Rammler, predict size distributions from experimental data [18]. Image-based techniques, favored for their efficiency, analyze fragmentation using software like SPLIT and WipFrag [8]. However, 2D imaging systems dominate most prior research, despite their limitations compared to emerging 3D imaging and laser scanning methods [19]-[21].

Recent advancements in machine learning (ML) have enhanced image-based fragmentation analysis. ML algorithms, used for pattern recognition, enable tasks like mineral grain classification and rock texture analysis [22]. For instance, Maitre *et al.* (2019) achieved 90% accuracy in sand grain recognition using ML [23]. Similarly, Tessier (2007) and Perez (2011) developed models to predict rock properties and ore grades, respectively, leveraging machine vision [24] [25]. Yaghoobi *et al.* (2019) introduced a neural network-based classification algorithm for fragmentation assessment, though its accuracy was limited to 67% due to a focus on textural features [26].

Despite the potential of empirical, observational, and image-based techniques, they are potential to face challenges. Sieving is laborious and unsuitable for large-scale muck piles [8]. Observational methods suffer from subjectivity, and image-based techniques encounter errors like particle delineation and sampling bias [1] [7]. Most ML models emphasize textural features, neglecting morphological characteristics essential for fragmentation assessment [3] [6].

In this study, a new ML-based classification method was developed to evaluate

rock fragmentation in a sublevel caving (SLC) mine. Using images of loaded LHD buckets, fragments were categorized into five classes, from fine material to boulders. Data were collected over a year to minimize sampling bias and improve reliability. This method focuses on extracting morphological features, addressing limitations in previous studies. By analyzing surface fragments visible in images and identifying boulders distinctly, the model offers an efficient and accurate solution for fragmentation assessment in SLC mining operations.

2. Methodology

This research involves a comprehensive literature review, data collection and model development. Figure 1 shows a schematic diagram of the research methodology.

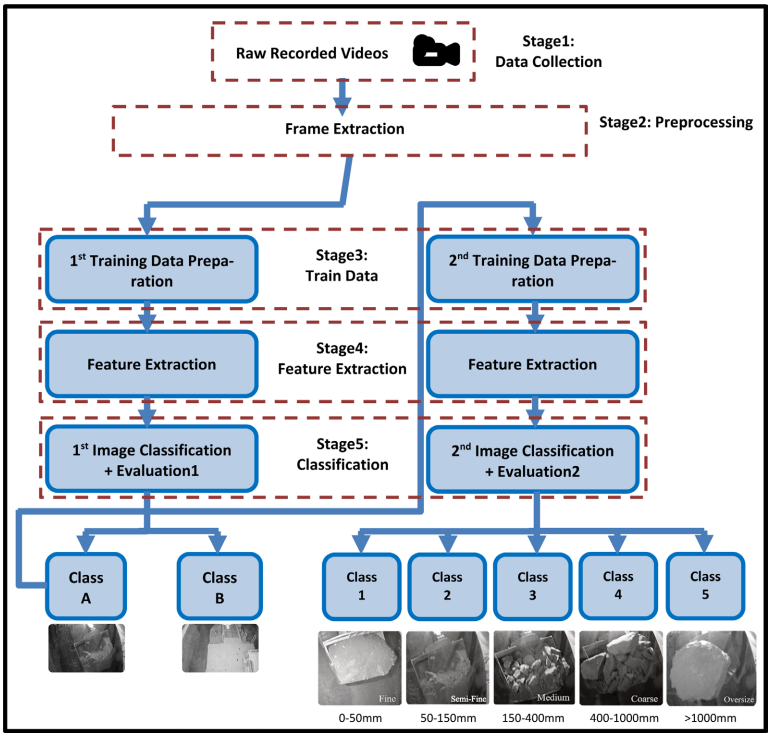

Figure 1. Research methodology.

2.1. Data Collection

Malmberget iron ore mine owned and operated by LKAB is in Gällivare municipality, 120 km to the South from Kiirunavaara in northern Sweden [27]. It consists of 20 ore bodies, which spread over a large underground area of 2.5 by 5 km [28]. Input data for this research were collected from one of the orebodies in the mine at a production level of 1052 m. To record the whole loading operation from two productions drifts o4930 and o4960; two cameras with a frame rate of 30 fps were installed at the entrance of each drift. The cameras were configured to record a short video whenever there was a movement in the recording area to get the required images for the fragmentation assessment. To record high quality videos for further processing, the cameras were assisted with proper lighting conditions.

However, dust in an underground environment always tends to reduce the quality of the recording; it did not affect the analysis by applying noise removing filters on the images as a pre-processing step. The headlights of the LHD machines sometimes caused problems and distortion of the frame pixels. Hence the cameras and mounted lights were aligned to reduce the undesired light effects. This recording procedure lasted for more than a year, which resulted in videos of more than 10,000 LHD buckets filled with blasted ore.

2.2. Frame Extraction

In the frame extraction step, the maximum possible number of frames were extracted from the videos. Each video produced around 600 - 1200 frames depending on the length of the video. Since motion detector cameras were utilized to record videos, the extracted frames showed distinct images. Empty frames (e.g., **Figure 2(a)**), indicate that the LHD vehicle had not passed yet, or in some cases, it was the LHD front lights that triggered the sensor. In addition, some frames include vehicles other than LHDs (e.g., staff vehicles, service vehicles, etc. **Figure 2(b)** and **Figure 2(c)**). Empty LHD buckets could also be seen in some frames (e.g., **Figure 2(d)**). Some frames are extracted while the other parts of LHD except the loaded bucket is in front of the camera which is not required for analysis (e.g., **Figure 2(e)** and **Figure 2(f)**). Among all the frames in **Figure 2**, the only ones on which the analytics methods could be applied are **Figure 2(g)** and **Figure 2(h)**. Therefore, refining the extracted frames and keeping those with the fully loaded LHD buckets was necessary. In this case, the first classifier has been developed, which categorizes the full bucket LHD from other frames. One of the major differences in this research compared to the study conducted by S. Manzoor (*et al.*) is that all the steps in this research is done automatically using the codes implemented using Python and Matlab [29]. While in the study done by S. Manzoor (*et al.*) the required frames are separated from the others manually which is a bottleneck. Manually classification of the frames to be required and not required

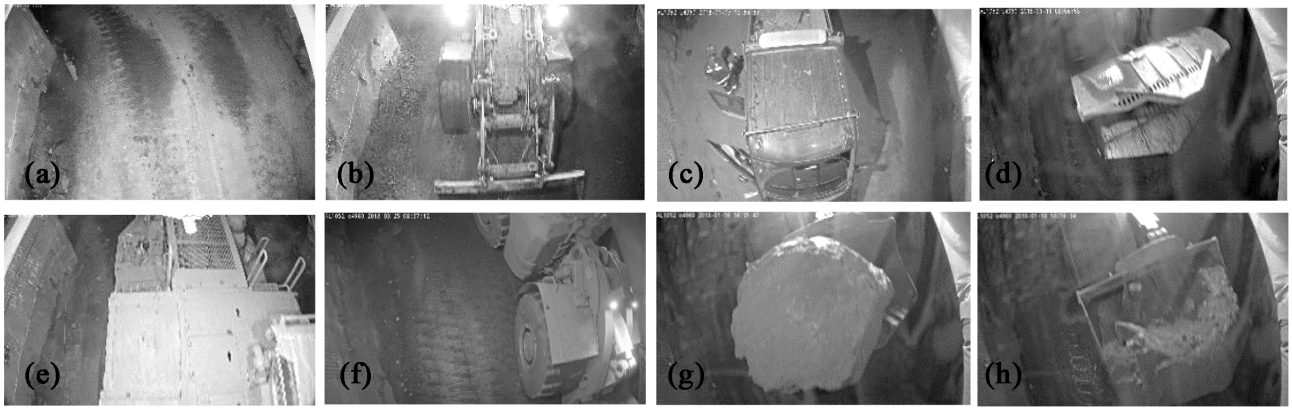

Figure 2. Different Types of Image Frames Extracted from Recorded videos. [(a) Empty, (b) and (c) Vehicles other than LHDs, (d) Empty LHD buckets, (e) and (f) other parts of LHD except the loaded bucket, (g) and (h) loaded bucket of LHD] (Images are published on [29]).

groups is more expensive and time consuming since a human need to be paid to classify the frames, and it takes longer time to be finalized than classifying them automatically on the computer. In the following, the first high classifier to extract the required frames is explained in more details.

2.3. Training Data Preparation for First Classification

The training data for the first classifier was prepared with visual observations. The extracted frames from different videos were manually evaluated and separated into "Class A" and "Class B". Class A consists of the frames with images of loaded buckets, while Class B covers the rest of the frames. It was important to include all sorts of frames with distinct types of information in the training data to accommodate the variation in data and achieve higher accuracy.

2.4. Training Data Preparation for Second Classification

To prepare the training data for the second step of model development, Split-Desktop was used to evaluate fragmentation from the extracted images of the LHD buckets. The system uses digital images to measure the rock fragment size distribution. It was used to analyze the extracted frames with LHD buckets containing rock pieces and follow the procedure described by Bobo [30]. The first step involves setting up the scale for each image to reference the fragment size calculations. Fragments in the image are automatically delineated in the second step. In the third step, this automatic delineation of the fragments is later manually edited to improve the accuracy of the results. The fourth step calculates the fragment size distribution from the image. The results can be displayed with different graphing and display options in the last step. In this study, the fragment size distribution was based on median size (50×) *i.e.*, the mesh size at which at least 50% of the material would pass through it.

2.5. Feature Extraction

Feature extraction is the key step in image analysis using computer vision. It highly affects the accuracy of image classification. In this stage, the main goal is to extract a set of informative features concerning the desired properties of input data. Therefore, a feature extractor reduces the number of variables required to describe a large set of data. Bag-of-visual-features (BoVF) is a current feature extraction method that uses the same path as the bag-of-words method in text processing by considering image features as words [31]-[34]. In this method, a histogram of a visual vocabulary was formed from local visual features. In the first step, feature descriptors were identified by feature sampling from input images and later created a visual vocabulary. In the next step, the extracted feature descriptors were grouped into some mutually exclusive clusters using the k-means clustering algorithm. Using k-means, each descriptor was assigned to the cluster with the nearest mean as a cluster prototype [35].

In this case, each cluster means a visual codeword. The frequency of the

assigned code words for each image shows the feature vector. Figure 3 represents the mentioned steps of the feature extraction method. This research used the Speeded Up Robust Features (SURF) detector to select the informative scale-invariant features [36]. This method is inspired by the scale-invariant feature transform (SIFT) descriptor, but it is several times faster and more robust against image transformations than SIFT. SURF is a feature extraction algorithm commonly used in computer vision and image processing tasks. The SURF algorithm is based on the concept of interest points, which are distinctive locations in an image that can be robustly detected and described. These interest points are usually located at corners, blobs, or regions with significant texture variations. The main steps involved in the SURF algorithm are scale-space extrema detection, key point localization, orientation assignment, descriptor computation, and feature matching.

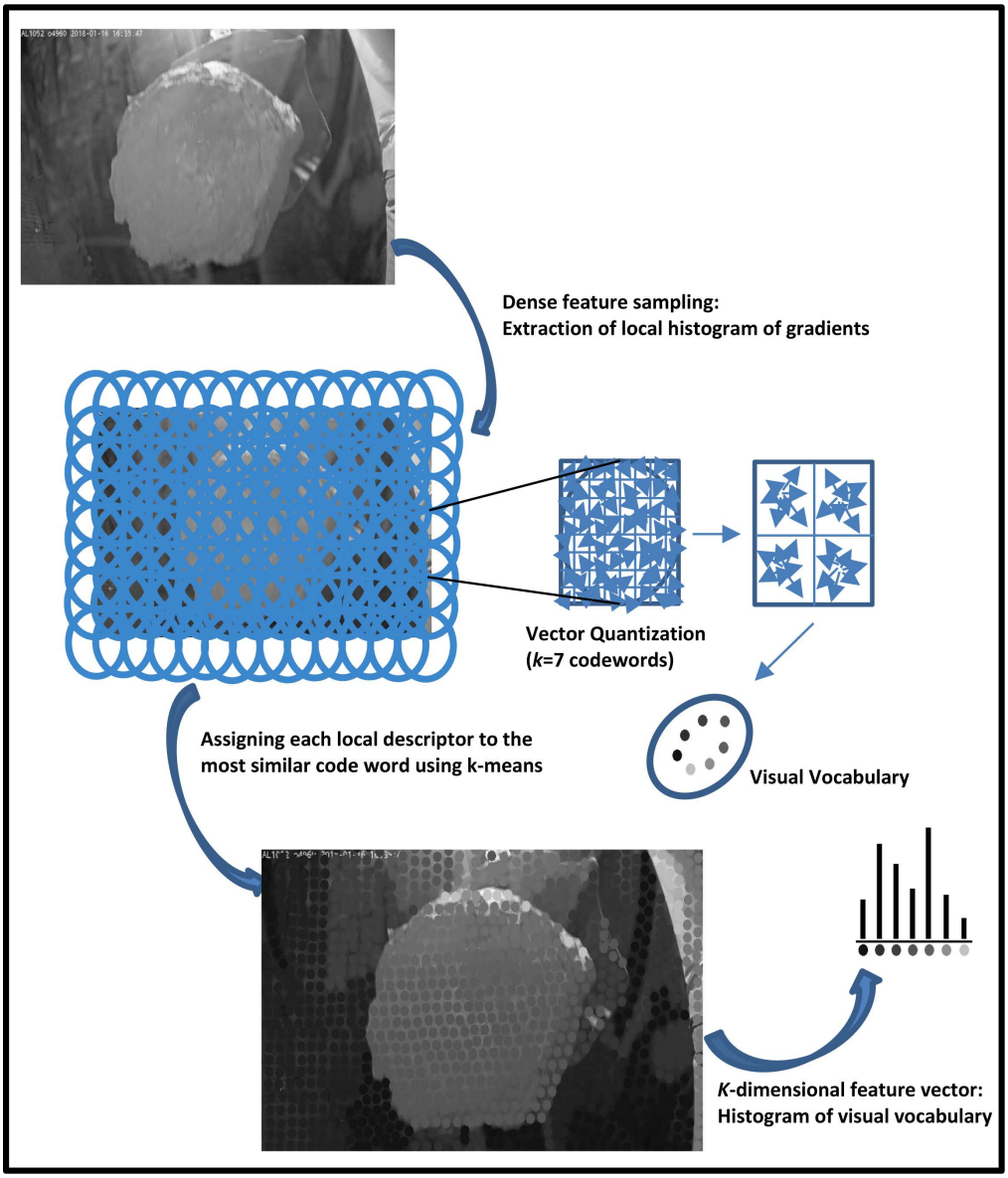

Figure 3. Bag of words feature extraction method.

SURF uses the determinant of Hessian blob to detect interest points. In addition, the region of interest is identified based on the sum of the Haar wavelet response. Overall, SURF is a popular feature extraction algorithm that offers a good balance between speed and accuracy, making it suitable for various computer vision applications.

2.6. First Image Classification

As mentioned earlier, Class A consisted of the frames that had images of loaded buckets, *i.e.*, buckets containing rock material. All the other frames, which had images with another information rather than loaded buckets, were classified as "Class B". Frames extracted from the videos recorded while an LHD with an empty bucket passed through the camera or the videos recorded because of other moving objects/vehicles are examples from Class B. Existing noisy videos might affect the classification accuracy. Noise effects were eliminated by extracting up to three frames from each video in this classification step. The reason of choosing up to three frames is that in the next step, the class of each video is specified by applying majority vote technique. Since it is not desired that the voting leads to an equal result, the number of selected frames must be odd. In addition, as the number of selected frame's increases, the number of size classification of frame's increases too. Hence, for a large number of frames, the size classification step would be time consuming. In order to avoid the complexity, the smallest, odd number greater than 1 is selected, and that number is three. If there was any frame belonging to Class "A" for each video, only up to three with the highest quality were saved for further analysis. This increased the probability of selecting the least noisy frames if the noise occurred while the loaded bucket of LHD was passing in front of the camera. Furthermore, since noises increase the complexity of the fragment size analysis, the achieved results from these three frames have been combined to provide a higher classification accuracy. Combining results from three frames to accomplish the last fragmentation class was also fruitful for noise-free videos. In this case, if there was more than one class for a certain video, the most relevant class could be assigned using the voting method. For example, in **Figure 2**, **Figure 2(c)** and **Figure 2(d)** belong to "Class A" while the rest belongs to "Class B". If all the extracted frames were used for fragmentation classification, it would result in a complicated scenario, producing inefficient results. This stage was performed to discard those extracted frames that do not possess any relevant information on the fragmentation classification. In this study, the first stage classification produces the data required for fragmentation classification, and the irrelevant data is discarded.

2.7. Second Image Classification

In the second stage of classification data from class, "A" was subdivided into five classes entitled "Class 1", "Class 2", "Class 3", "Class 4" and "Class 5" depending on 50× of the loaded material in the bucket.

Class 1 contains the images with median particle size (50×) of rock material less than 50 mm. It means that the material shown in the image has at least 50% material with size less than 50 mm. Class 2 contains images with 50×, which ranges in 50 - 150 mm. Class 3 contains images with 50×, which ranges in 150 - 400 mm. Class 4 contains images with 50×, which ranges in 400 - 1000 mm, and Class 5 contains images with 50× > 1000 mm. Based on the mentioned sizes, this classification has been utilized by Danielsson *et al.* [22].

In this step, each of the extracted frames from a video is classified separately into one of the five classes. Then, the last class based on the median particle size was assigned to the related video using the result of the majority vote on the classes assigned to the three frames. Figure 4 shows how the majority vote method is applied in this study. For Video 1, all three frames are classified as Class 1; Consequently, Class 1 should be assigned to the related video. For Video 2, two of the frames are identified as Class 5, while one of them is from Class 4. In this case, the video is considered Class 5 based on the majority vote.

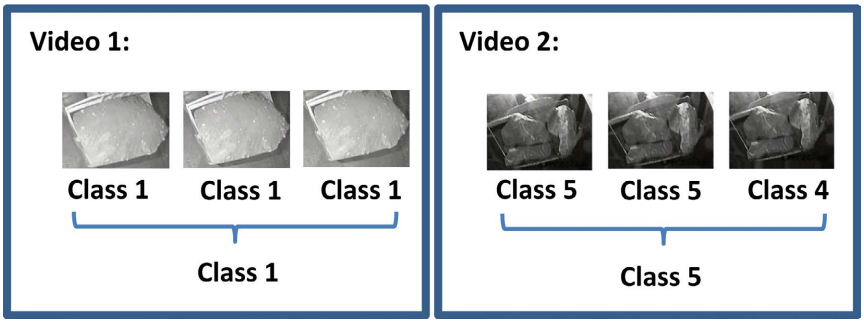

Figure 4. The fragmentation class is assigned to each video by combining the results of related (Rock images are published on [29]).

2.8. Classification Modeling

In machine learning and statistics, classification is a supervised learning approach. The computer program learns from the input data and then uses this learning to classify new observations [37]. This data set may be bi-class or multi-class. Distinct data types (e.g., signals, texts, images, etc.) could be considered the input in a classification problem. In this research, there were two steps of image classification. The extracted frames from recorded videos and the histogram of their visual features achieved by a SURF-based bag of visual words were used for training the models. The classification methods which were tested during this study are briefly described as follows:

2.8.1. Support Vector Machines (SVMs)

Support-vector machines are considered as a "supervised" machine-learning model, meaning that the input data should be assigned by "labels" [38]. The classification in the method is formed by mapping y (x, w), which illustrates a map from input x to output. Moreover, all the control of mapping is handled by weights. SVM, like other methods, has two significant steps: the training step and the inferencing

one. Training data are used to estimate the parameters and hyperparameters vectors in the training step. Then, in the inference step, the training data are discarded and predicted for a new dataset (*i.e.*, unseen dataset by the trained model) is carried out based on the learned parameters and hyperparameters. However, some machine learning methods are widely used for training datasets since the aim is pattern recognition. In pattern recognition, prediction is based upon the similarity of the test data set for the training set. For instance, nearest neighbors, which are explained in the following section, are an excellent example of such methods that utilize the training dataset in the inference step. Since the nearest neighbor methods require comparing training and test data sets, they are called memory-based methods. Therefore, the major disadvantage of memory-based methods is time inefficiency when working with high-volume datasets.

For the first classification in this study, these labels are class "A" and class "B". For a given set of training data, and each frame was marked with the proper label. Then the labeled data were used as the input kernel based SVM model. The method was supposed to separate the two mentioned categories to maximize the discriminative model and support vector's gap. Corinna and Vladimir (1995) presented a detailed explanation of the SVM method. To improve the model's accuracy in identifying complex dependencies between features of the samples, the kernel trick is often used in the SVM method [39]. Kernel trick means operating in a high-dimensional and implicit feature space without computing the coordinates of the data in that space, but by simply computing the inner products between all pairs of images in the feature space. Gaussian kernel was used for this research to consider the samples in infinite dimension space. In the first classification phase, kernel based SVM for binary classification led to the most accurate result to classify the extracted frames into two classes "A" and "B". SVM method can also be applied to datasets with more than two classes using one vs. rest technique [40]. Using this technique, one class is separated from the others in each stage, and the problem is solved as a binary classification problem. In the end, the results from different steps are combined to obtain the last result.

2.8.2. Ensemble Learning

To obtain better predictive performance than the constituent learning algorithms alone, "ensemble method" employ multiple learning algorithms instead [41]. Combination of diverse weak learners improves the accuracy and stability of the analysis [42]. Bagging, boosting, and stacking are the most common ensemble learning techniques. In the bagging technique, similar learners are developed based on a random subset of the samples and named weak learners. Next, the predictions of these classifiers are combined. The main data are first partitioned into different subsets to apply this technique. Then each weak learner is trained based on the input data subset. Finally, the predictions from weak learners are combined to obtain a predicted value on a considered parameter. In this research, bagging based on k-nearest neighbors led to the highest accuracy to classify the frames in class "A" to five different classes based on median particle size. In addition, the

results from bagging trees were compared with the others which led to the least accuracy among the other applied techniques.

2.8.3. K-Nearest Neighbours (KNN)

K-nearest neighbor is a non-parametric method used for classification and regression in pattern recognition [43]. As a classification method, the output is a class membership. An object is classified considering the majority vote of its neighbors, with the object being assigned to the class most common among its k nearest neighbors. In the second classification step of this study, the bag of KNNs led to the highest accuracy of 89.9%.

2.8.4. Decision Trees

A decision tree is a pattern recognition tool that uses a tree-like model of different states and their consequences for classification [44]. Each internal node of this structure represents a test on a feature while each leaf node implies a class. In each classification step of this research, bagging based on decision trees as weak learner was tested [45]. As shown in the last column of **Table 1** and **Table 2**, decision trees did not provide the highest accuracy in the above-mentioned classifications in this study.

2.9. K-Fold Cross-Validation

Cross-validation or out-of-sample testing is a model validation technique to test the model's ability to predict new data that was not used in the model development [46]. Moreover, it gives an insight into how the model will generalize to an independent dataset. The procedure has a single parameter called k that implies the number of groups in which a given data sample should be split. As such, the process is often called k-fold cross-validation. Both classification models were developed using a 5-fold cross validation method in this research, which is a popular variant of k-fold cross-validation. In each classification stage, five models were obtained, and each one was tested based on one-fifth of the sample population. The final accuracy was achieved by combining the results from five models.

3. Result and Discussion

As mentioned above, image classification was carried out in two steps. Kernel based SVM and ensemble-learning methods based on KNN, and decision tree were employed in both classification steps, and the obtained results were compared to find the best classification method. Since computer memory can process a specific data size, 7500 videos were used in this study to train the models considering the utilized memory. After that, the frames were extracted and classified into the earlier described two classes "A" and "B". The accuracies for the first image classification phase are shown in **Table 1**. It shows that the Kernel based SVM had a bit higher accuracy in average compared with the Ensemble learning, 99.8% and 98.9% respectively.

Since many frames with no loaded LHD buckets were placed in class B, this

Table 1. Results for the first image classification phase.

1st Classification	Kernel based SVM	Ensemble Learning (Bagging KNN)	Ensemble Learning (Bagging Trees)
Accuracy, % (5-fold cross validation)	99.8 ± 0.1	98.9 ± 0.8	90.1 ± 2.1

class included an enormous number of data, which produces high variance. At the same time, class A included only the frames showing loaded LHD buckets and had much less variance. Using SVM, a discriminative model was developed to maximize the gap between the two classes. This gap causes generalizability in the model regarding a wide variety of data in Class B.; Accordingly, it can avoid misclassification for the high variance input data. In addition, using the kernel trick could clarify the complex dependencies. This would therefore lead to more accurate classification. Here, the Gaussian kernel has considered the samples in infinity dimension space and the complex relations between the samples were evaluated. Hence, as shown in Table 1, the kernel based SVM has led to the highest average accuracy in this binary classification step. The achieved result based on bagging KNN was close to that of SVM and even overlapped the standard deviations. This shows that combining the results from different tuned non-parametric KNN models also led to acceptable accuracy. In this study, there were a lot of input data covering the diversity of the problem space. Since KNN classifies the input data regarding the properties of samples in the neighborhood, there were enough input samples. Therefore, the bagging KNN led to this step's second highest average accuracy. In addition, bagging KNN improved accuracy due to the ensemble learning technique's properties. Bagging trees method has the third place among the measured accuracies. However, this technique is limited to the dimensions in the original space, and it cannot consider the complexity of dependencies among the samples. Therefore, there is a considerable difference between the accuracies from the other two techniques.

In the second step of classification, frames selected as Class A in the previous step were processed by exploiting the three mentioned classification techniques. Table 2 represents the accuracy of the second image classification phase.

Table 2. Result of second image classification phase.

1st Classification	Kernel based SVM (One vs. Rest)	Ensemble Learning (Bagging KNN)	Ensemble Learning (Bagging Trees)
Accuracy, % (5-fold cross validation)	87.8 ± 0.6	89.8 ± 0.5	83.7 ± 1.3

Bagging KNN led to an average accuracy of 89.8% in the second phase of the image classification. This step extracts up to three frames from each video with loaded LHD used as the input data. Each frame is classified into one of the five classes based on the median fragment size. As mentioned previously, the best

three frames were extracted from each video containing a loaded bucket. Here, the class of each video was recognized by considering the majority vote. One of the fragmentation classes was selected based on the majority of votes to classify the video. The mentioned accuracy shows that 89.8% of these videos were classified correctly based on median fragment size. Since different KNN models are trained based on other random parts of the samples, each model covers a portion of data, and the result is the combination of those obtained from different models. As presented earlier, enough input samples are appropriately expanded in the problem space. Hence, the non-parametric KNN model is strong enough to cover the complexities of different sample parts. This explains why bagging KNN obtained the highest accuracy in this step. However, the kernel based SVM method is designed for binary classification; it was applied to five classes in this study by applying "one vs. rest" technique. The result achieved using kernel based SVM was close to the bagging KNN, which showed that considering dependencies in high dimension space and applying SVM to develop a discriminative model could obtain an acceptable result. It should be noted that the bagging trees' method was limited to the dimensions in the original space, which could explain the considerable difference concerning accuracy compared with the other tested techniques.

The proposed method achieves a fragmentation classification accuracy of 89.8%, significantly outperforming the 67% accuracy reported in other research utilizing a neural network-based classification algorithm [26]. In addition, the proposed method achieves a fragmentation classification accuracy of 89.8% without requiring GPU resources or complex training processes. In comparison, other research utilizing a high-complexity CNN deep learning network reported a slightly higher accuracy of 93.78% [47]. However, this increased accuracy comes at the cost of significantly higher resource requirements for model training, as well as a more time-intensive and computationally expensive training process. The lower accuracy in the previous approach is attributed to its reliance on textural features, whereas the proposed method leverages more effective extracted features, resulting in improved performance. In this research, the classification is done automatically, and the processing speed has been increased compared to software-based fragmentation classification such as Split-Desktop. The quality of images taken in an underground environment as well as during the movement of LHDs also limits the use of any such software [48]. Even if the image quality is enhanced by applying filters like "Unsharp Mask" in Split-Desktop, the particle delineation is always user-biased and needs 10 - 15 minutes per image [48]. A complete manual particle delineation can take up to 2 hours per image using Split-Desktop. In addition, it has been figured out that processing and manual classification by looking at every video and classifying it into any of the fragmentation classes took 89 seconds on average per video while the average required time for the proposed method is 75 seconds. Although the time difference between the proposed and the manual classification looks small, *i.e.*, 14 seconds, there are still at least three benefits of the proposed technique.

Table 3. Comparison of the proposed method, split-desktop, and manual classification for fragmentation analysis.

Aspect	Proposed Method	Split-Desktop	Manual Classification
Automation	Fully automatic classification; does not require user intervention.	Requires user input and manual particle delineation, making it time-consuming.	Requires manual observation and user effort to classify each video, leading to potential fatigue and inconsistency.
Processing Time	Faster processing (75 seconds per video on average).	Manual particle delineation takes 10 - 15 minutes per image with filters like "Unsharp Mask" and up to 2 hours per image manually.	Average processing time is 89 seconds per video, which is slower than the proposed method.
Scalability	Capable of handling thousands of videos efficiently; saves significant time in bulk processing.	Not scalable due to extensive manual effort required for each image or video.	Limited scalability; analyzing 10,000 videos would take 41.67 more hours compared to the proposed method.
Accuracy	High accuracy; free from user bias and experience dependence.	Accuracy depends heavily on user experience and manual particle delineation.	Observational method prone to high inaccuracies due to user experience and bias.
Cost	Cost-free once deployed; no subscription fees.	Subscription-based online processing packages for continuous monitoring are costly and create financial barriers.	Involves indirect costs like human resource allocation for manual analysis.
Suitability for Poor Image Quality	Affected by poor image quality but still effective for images taken in challenging environments such as underground or during LHD movement.	Limited by image quality, requiring additional preprocessing like applying filters, which may not fully resolve the challenges.	Affected by poor image quality; manual observations are harder and more error-prone in such conditions.

Based on the comparison in the Table 3, the proposed method is both time-efficient and cost-effective for fragmentation classification, especially in scenarios requiring continuous monitoring. The probability of correctly classifying a video using the developed two-step framework is the joint probability of success in the binary classification step and the subsequent assignment of an appropriate fragmentation class. As shown in Table 1 and Table 2, the probabilities for these two steps are 0.998 and 0.898, respectively, resulting in an overall classification accuracy

of 89.62% for videos based on median fragment size. While software such as Split-Desktop is reputed for higher accuracy, its performance heavily relies on user experience in particle delineation. Moreover, subscription-based online processing packages for continuous monitoring are costly and present a significant financial barrier. In contrast, the proposed fully automatic method, once deployed, is cost-free and readily scalable for online processing of fragmentation. Additionally, this method demonstrates superior classification accuracy compared to prior artificial intelligence-based techniques by leveraging the shape-expressive features of image elements. These advantages, combined with the reduced computational costs and enhanced time efficiency, underscore the practicality and superiority of the proposed approach for real-world applications.

A potential challenge in applying the proposed method across different mining environments lies in the variability of environmental conditions such as lighting, dust, and movement. However, the method is designed to overcome these challenges by operating on recorded videos rather than single images, automatically extracting the most suitable frame for analysis. As long as one recognizable frame can be extracted—where "recognizable" means that a human can discern fragment boundaries despite environmental conditions—the method remains effective. This adaptability highlights the generalizability of the proposed approach, ensuring consistent performance across different environments. Although the research was conducted using data extracted from a single mine, the method is equally applicable to rock fragment images from other mines, as its performance is not mine-specific. From an implementation perspective, the method requires no costly hardware, software, or computational resources; once deployed, it is entirely free to use. While the method performs robustly with the existing setup, there is room for improvement in accuracy through the use of deep learning techniques. These methods, while more accurate, would necessitate investing in GPU hardware or cloud-based GPU resources, presenting a trade-off between accuracy and cost. Overall, the proposed method strikes a balance between reliability, cost-efficiency, and adaptability to diverse mining conditions, making it practical for widespread application.

4. Conclusion

Increasing the amount of image data can reduce the sampling errors in fragmentation assessment but requires a significant amount of time to analyze those images. In some cases, it becomes impractical to analyze data manually because of the extensive amounts of data. Hence, in this study, an image analysis technique based on machine learning algorithms is developed to classify rock fragmentation in different classes to remove the time constraints. The proposed method shows higher accuracy compared to the previous automatic techniques. Moreover, as the future work, this developed framework could analyze the effect of different blast hole sizes on rock fragmentation and identify any relationship between measurement while drilling and rock fragmentation in sublevel caving mines in the future.

However, more features could be considered in the feature selection method in future works to increase the classification accuracy. For example, camera inspections will be helpful to reduce noisy footage. Lighting in the video recording area is also an important parameter that affects the results. Appropriate lighting increases the visibility of the rock fragments in the LHD bucket and, therefore, increases its classification accuracy.

Statement and Declarations

This work was supported by LKAB and the management and staff of Malmberget. This study was funded by Center for Advanced Mining and Metallurgy (CAMM2). In addition, the research leading to these results received funding from Vinnova, the Swedish Energy Agency and Formas through the SIP-STRIM program.

Conflicts of Interest

The authors declare no conflicts of interest regarding the publication of this paper.

References

[1] Bamford, T., Esmaeili, K. and Schoellig, A.P. (2017) A Real-Time Analysis of Post-Blast Rock Fragmentation Using UAV Technology. *International Journal of Mining, Reclamation and Environment*, **31**, 439-456. https://doi.org/10.1080/17480930.2017.1339170

[2] Tavakol Elahi, A. and Hosseini, M. (2017) Analysis of Blasted Rocks Fragmentation Using Digital Image Processing (Case Study: Limestone Quarry of Abyek Cement Company). *International Journal of Geo-Engineering*, **8**, Article No. 16. https://doi.org/10.1186/s40703-017-0053-z

[3] Hunter, G.C., McDermott, C., Miles, N.J., Singh, A. and Scoble, M.J. (1990) A Review of Image Analysis Techniques for Measuring Blast Fragmentation. *Mining Science and Technology*, **11**, 19-36. https://doi.org/10.1016/0167-9031(90)80003-y

[4] Badroddin, M., Khoshrou, H. and Siamaki, A. (2013) Prediction of Fragment Size Distribution from Blasting: Artificial Neural Networks Approach. 36*th APCOM Symposium Applications of Computers and Operations Research in the Mineral Industry*, Porto Alegre, 4-8 November 2013.

[5] Cho, S.H. and Kaneko, K. (2004) Rock Fragmentation Control in Blasting. *Materials Transactions*, **45**, 1722-1730. https://doi.org/10.2320/matertrans.45.1722

[6] Kemeny, J.M., Devgan, A., Hagaman, R.M. and Wu, X. (1993) Analysis of Rock Fragmentation Using Digital Image Processing. *Journal of Geotechnical Engineering*, **119**, 1144-1160. https://doi.org/10.1061/(asce)0733-9410(1993)119:7(1144)

[7] Thurley, M.J. (2013) Automated Image Segmentation and Analysis of Rock Piles in an Open-Pit Mine. 2013 *International Conference on Digital Image Computing: Techniques and Applications* (*DICTA*), Hobart, 26-28 November 2013, 1-8. https://doi.org/10.1109/dicta.2013.6691484

[8] Siddiqui, F., Shah, S. and Behan, M. (2009) Measurement of Size Distribution of Blasted Rock Using Digital Image Processing. *Journal of King Abdulaziz University-Engineering Sciences*, **20**, 81-93. https://doi.org/10.4197/eng.20-2.4

[9] Seccatore, J. (2019) A Review of the Benefits for Comminution Circuits Offered by Rock Blasting. *REM—International Engineering Journal*, **72**, 141-146.

https://doi.org/10.1590/0370-44672017720125

[10] Onederra, I., Thurley, M.J. and Catalan, A. (2014) Measuring Blast Fragmentation at Esperanza Mine Using High-Resolution 3D Laser Scanning. *Mining Technology*, **124**, 34-36. https://doi.org/10.1179/1743286314y.0000000076

[11] Casali, A., Gonzalez, G., Vallebuona, G., Perez, C. and Vargas, R. (2001) Grindability Soft-Sensors Based on Lithological Composition and On-Line Measurements. *Minerals Engineering*, **14**, 689-700. https://doi.org/10.1016/s0892-6875(01)00065-6

[12] Roy, M.P., Paswan, R.K., Sarim, M.D., Kumar, S., Jha, R. and Singh, P.K. (2016) Rock Fragmentation by Blasting—A Review. *Journal of Mines, Metals and Fuels*, **64**, 424-431.

[13] Babaeian, M., Ataei, M., Sereshki, F., Sotoudeh, F. and Mohammadi, S. (2019) A New Framework for Evaluation of Rock Fragmentation in Open Pit Mines. *Journal of Rock Mechanics and Geotechnical Engineering*, **11**, 325-336. https://doi.org/10.1016/j.jrmge.2018.11.006

[14] Johansson, D. and Ouchterlony, F. (2011) Fragmentation in Small-Scale Confined Blasting. *International Journal of Mining and Mineral Engineering*, **3**, 72-94. https://doi.org/10.1504/ijmme.2011.041450

[15] Wimmer, M., Nordqvist, A.A., Ouchterlony, F. and Selldén, H. (2012) 3D Mapping of Sublevel Caving (SLC) Blast Rings and Ore Flow Disturbances in the LKAB Kiruna Mine. Luleå University of Technology.

[16] Sanchidrián, J.A., Ouchterlony, F., Segarra, P. and Moser, P. (2014) Size Distribution Functions for Rock Fragments. *International Journal of Rock Mechanics and Mining Sciences*, **71**, 381-394. https://doi.org/10.1016/j.ijrmms.2014.08.007

[17] Beyglou, A. (2017) Target Fragmentation for Efficient Loading and Crushing—The Aitik Case. *Journal of the Southern African Institute of Mining and Metallurgy*, **117**, 1053-1062. https://doi.org/10.17159/2411-9717/2017/v117n11a10

[18] Ouchterlony, F. (2009) Fragmentation Characterization; the Swebrec Function and Its Use in Blast Engineering. *Proceedings of the 9th International Symposium on Rock Fragmentation by Blasting*, Granada, 13-17 August 2009, 3-22.

[19] Chatterjee, S., Bhattacherjee, A., Samanta, B. and Pal, S.K. (2010) Image-Based Quality Monitoring System of Limestone Ore Grades. *Computers in Industry*, **61**, 391-408. https://doi.org/10.1016/j.compind.2009.10.003

[20] Gaich, A., Pötsch, M. and Schubert, W. (2017) Digital Rock Mass Characterization 2017—Where Are We Now? What Comes Next? *Geomechanics and Tunnelling*, **10**, 561-566. https://doi.org/10.1002/geot.201700036

[21] Campbell, A.D. and Thurley, M.J. (2017) Application of Laser Scanning to Measure Frag-Mentation in Underground Mines. *Mining Technology*, **126**, 240-247.

[22] Danielsson, M., Ghosh, R., Navarro Miguel, J., Johansson, D. and Schunnesson, H. (2017) Utilizing Production Data to Predict Operational Disturbances in Sublevel Caving. 26*th International Symposium on Mine Planning and Equipment Selection*, Luleå, 29-31 August 2017, 139-144.

[23] Maitre, J., Bouchard, K. and Bédard, L.P. (2019) Mineral Grains Recognition Using Computer Vision and Machine Learning. *Computers & Geosciences*, **130**, 84-93. https://doi.org/10.1016/j.cageo.2019.05.009

[24] Tessier, J., Duchesne, C. and Bartolacci, G. (2007) A Machine Vision Approach to On-Line Estimation of Run-Of-Mine Ore Composition on Conveyor Belts. *Minerals Engineering*, **20**, 1129-1144. https://doi.org/10.1016/j.mineng.2007.04.009

[25] Perez, C.A., Estévez, P.A., Vera, P.A., Castillo, L.E., Aravena, C.M., Schulz, D.A., *et*

al. (2011) Ore Grade Estimation by Feature Selection and Voting Using Boundary Detection in Digital Image Analysis. *International Journal of Mineral Processing*, **101**, 28-36. https://doi.org/10.1016/j.minpro.2011.07.008

[26] Yaghoobi, H., Mansouri, H., Ebrahimi Farsangi, M.A. and Nezamabadi-Pour, H. (2019) Determining the Fragmented Rock Size Distribution Using Textural Feature Extraction of Images. *Powder Technology*, **342**, 630-641. https://doi.org/10.1016/j.powtec.2018.10.006

[27] Danielsson, M., Söderström, E., Schunnesson, H., Gustafson, A., Fredriksson, H., Johansson, D., *et al*. (2022) Predicting Rock Fragmentation Based on Drill Monitoring: A Case Study from Malmberget Mine, Sweden. *Journal of the Southern African Institute of Mining and Metallurgy*, **122**, 1-11. https://doi.org/10.17159/2411-9717/1587/2022

[28] Ghosh, R., Danielsson, M., Gustafson, A., Falksund, H. and Schunnesson, H. (2017) Assessment of Rock Mass Quality Using Drill Monitoring Technique for Hydraulic ITH Drills. *International Journal of Mining and Mineral Engineering*, **8**, 169-186. https://doi.org/10.1504/ijmme.2017.085830

[29] Manzoor, S., Gustafson, A., Schunnesson, H., Tariq, M. and Wettainen, T. (2022) Rock Fragmentation Measurements in Sublevel Caving: Field Tests at LKAB's Malmberget Mine. In: Potvin, Y., Ed., *Caving* 2022: *Fifth International Conference on Block and Sublevel Caving*, Australian Centre for Geomechanics, 381-392. https://doi.org/10.36487/acg_repo/2205_26

[30] Bobo, T. (2010) What's New with the Digital Image Analysis Software Split-Desktop®? Split Engineering, LLC.

[31] Ohbuchi, R., Osada, K., Furuya, T. and Banno, T. (2008) Salient Local Visual Features for Shape Based 3D Model Retrieval. *Proceedings of IEEE Conference on Shape Modeling and Applications*, Stony Brook, 4-6 June 2008, 93-102.

[32] Ohbuchi, R. and Furuya, T. (2008) Accelerating Bag-of-Features Sift Algorithm for 3D Model Retrieval. *Proceedings of SAMT Workshop on Semantic* 3*D Media*, Koblenz, 3 December 2008, 23-30.

[33] Gao, Y. and Dai, Q. (2015) View-Based 3-D Object Retrieval. Morgan Kaufmann. 67-83.

[34] Furuya, T. and Ohbuchi, R. (2009) Dense Sampling and Fast Encoding for 3D Model Retrieval Using Bag-of-Visual Features. *Proceedings of the ACM International Conference on Image and Video Retrieval*, Santorini Island, 8-10 July 2009, 1-8. https://doi.org/10.1145/1646396.1646430

[35] Wagstaff, K., Cardie, C., Rogers, S. and Schrödl, S. (2001) Constrained k-Means Clustering with Background Knowledge. *International Conference on Machine Learning*, **1**, 577-584.

[36] Bay, H., Tuytelaars, T. and Van Gool, L. (2006) SURF: Speeded up Robust Features. In: Leonardis, A., Bischof, H. and Pinz, A., Eds., *Computer Vision—ECCV* 2006, 404-417. https://doi.org/10.1007/11744023_32

[37] Nikam, S.S. (2015) A Comparative Study of Classification Techniques in Data Mining Algorithms. *Oriental Journal of Computer Science & Technology*, **8**, 13-19.

[38] Cortes, C. and Vapnik, V. (1995) Support-vector Networks. *Machine Learning*, **20**, 273-297. https://doi.org/10.1007/bf00994018

[39] Theodoridis, S. and Koutroumbas, K. (2008) Pattern Recognition. Fourth Edition, Elsevier.

[40] Bishop, C.M. (2006) Pattern Recognition and Machine Learning. Springer Science+

Business Media.

[41] Rokach, L. (2009) Ensemble-Based Classifiers. *Artificial Intelligence Review*, **33**, 1-39. https://doi.org/10.1007/s10462-009-9124-7

[42] Ho, T.K. (1998) The Random Subspace Method for Constructing Decision Forests. *IEEE Transactions on Pattern Analysis and Machine Intelligence*, **20**, 832-844. https://doi.org/10.1109/34.709601

[43] Altman, N.S. (1992) An Introduction to Kernel and Nearest-Neighbor Nonparametric Regression. *The American Statistician*, **46**, 175-185. https://doi.org/10.1080/00031305.1992.10475879

[44] Magerman, D.M. (1995) Statistical Decision-Tree Models for Parsing. *Proceedings of the* 33*rd Annual Meeting on Association for Computational Linguistics*, Cambridge, 26-30 June 1995, 276-283. https://doi.org/10.3115/981658.981695

[45] Kamiński, B., Jakubczyk, M. and Szufel, P. (2017) A Framework for Sensitivity Analysis of Decision Trees. *Central European Journal of Operations Research*, **26**, 135-159. https://doi.org/10.1007/s10100-017-0479-6

[46] Cawley, G.C. and Talbot, N.L. (2010) On Over-Fitting in Model Selection and Subsequent Selection Bias in Performance Evaluation. *Journal of Machine Learning Research*, **11**, 2079-2107.

[47] Yang, Z., He, B., Liu, Y., Wang, D. and Zhu, G. (2021) Classification of Rock Fragments Produced by Tunnel Boring Machine Using Convolutional Neural Networks. *Automation in Construction*, **125**, Article ID: 103612. https://doi.org/10.1016/j.autcon.2021.103612

[48] Wimmer, M., Nordqvist, A., Righetti, E., Petropoulos, N. and Thurley, M. (2015) Analysis of Rock Fragmentation and Its Effect on Gravity Flow at the Kiruna Sublevel Caving Mine. *International Symposium on Rock Fragmentation by Blasting*, Sydney, 24-26 August 2015, 775-791.